



Groundwater vulnerability maps derived from a time-dependent method using satellite scatterometer data

Stefania Stevenazzi · Marco Masetti · Son V. Nghiem · Alessandro Sorichetta

Abstract Introducing the time variable in groundwater vulnerability assessment is an innovative approach to study the evolution of contamination by non-point sources and to forecast future trends. This requires a determination of the relationship between temporal changes in groundwater contamination and in land use. Such effort will enable breakthrough advances in mapping hazardous areas, and in assessing the efficacy of land-use planning for groundwater protection. Through a Bayesian spatial statistical approach, time-dependent vulnerability maps are derived by using hydrogeological variables together with three different time-dependent datasets: population density, high-resolution urban survey, and satellite QuikSCAT (QSCAT) data processed with the innovative dense sampling method (DSM). This approach is demonstrated extensively over the Po Plain in Lombardy region (northern Italy). Calibrated and validated maps show physically consistent relations between the hydrogeological variables and nitrate trends. The results indicate that changes of urban nitrate sources are strongly related to groundwater deterioration. Among the different datasets, QSCAT-DSM is proven to be the most efficient dataset to represent urban nitrate sources of contamination, with major advantages: a worldwide coverage, a continuous decadal data collection,

and an adequate resolution without spatial gaps. This study presents a successful approach that, for the first time, allows the inclusion of the time dimension in groundwater vulnerability assessment by using innovative satellite remote sensing data for quantitative statistical analyses of groundwater quality changes.

Keywords Vulnerability mapping · Urban areas · Remote sensing · Nitrate · Italy

Introduction

Groundwater is among the most important freshwater resources. In Western Europe, it contributes 60 % of the drinking-water supply (EuroGeoSurveys 2014). Increasing numbers of contamination sources in developed and developing countries critically threaten groundwater resources. Reactive remediation measures can be excessively expensive when groundwater becomes contaminated beyond the required quality standards for safe consumption.

Groundwater vulnerability studies are crucial to understand the cause-effect relationship between groundwater quality and both natural and anthropogenic factors to develop effective groundwater protection plans. Mapping areas where groundwater is most vulnerable to contamination and identifying primary factors influencing the contamination level are imperative to manage and protect groundwater and, thus, human health.

As groundwater resources have become more vulnerable in recent years, it is necessary to urgently close the gap between the information required for land use planning to efficiently safeguard groundwater quality and techniques required to accurately assess groundwater vulnerability. In fact, the European Union (EU) Groundwater Directive (2006/118/EC; European Community 2006) requires the identification of areas where groundwater suffers increasing trends in contaminant concentration, highlighting the need to carefully manage such areas even if the concentration is below the regulatory limit.

A current limitation in groundwater vulnerability studies is related to the lack of consideration of temporal trends (Stuart et al. 2007), and this emphasizes the need to consider the time dimension in assessing groundwater vulnerability. Methods currently used to assess groundwater

Received: 5 August 2014 / Accepted: 29 January 2015
Published online: 19 March 2015

© Springer-Verlag Berlin Heidelberg 2015

S. Stevenazzi (✉) · M. Masetti
Dipartimento di Scienze della Terra “A. Desio”,
Università degli Studi di Milano, Via Luigi Mangiagalli, 34, Milan,
20133, Italy
e-mail: stefania.stevenazzi@unimi.it

M. Masetti
e-mail: marco.masetti@unimi.it

S. V. Nghiem
Jet Propulsion Laboratory,
California Institute of Technology, 4800 Oak Grove Drive,
MS 300-235, Pasadena, CA 91109, USA
e-mail: son.v.nghiem@jpl.nasa.gov

A. Sorichetta
Geography and Environment,
University of Southampton, Highfield Campus, Shackleton
Building 44, Southampton, SO17 1BJ, UK
e-mail: A.Sorichetta@soton.ac.uk

vulnerability at a regional scale (Focazio et al. 2002) can be subjective (i.e., knowledge-driven) or objective (i.e., data driven). Subjective methods include overlay and index methods (e.g., DRASTIC, Aller et al. 1987; GOD, Foster 1987; AVI, Van Stempvoort et al. 1993; and EPIK, Doerflinger and Zwahlen 1997) and their modifications (Sener and Davraz 2013). They are easy to implement and require a limited amount of data to derive a subjective categorization of groundwater vulnerability. On the other hand, objective methods are based on the use of statistical methods, ranging from descriptive statistics (e.g., Welch et al. 2000) to regression and conditional probability analyses (e.g., Eckardt and Stackelberg 1995; Tesoriero and Voss 1997; Nolan 2001; Alberti et al. 2001; Worrall and Besien 2005; Masetti et al. 2009), which allow an objective determination of relations between the predictor factors and the level of contamination in the study area. In this regard, only objective methods allow scientifically defensible end products (Focazio et al. 2002) and, most importantly, enable an explicit integration of the time dimension in the groundwater vulnerability assessment (Sorichetta 2011).

Objective methods, however, face a major challenge that requires an extensive dataset, including a series of contaminant concentration measurements and natural and anthropogenic variables, to be consistent both in space and in time (Brunner et al. 2007). Addressing such a challenge demands a determination of the relationship between temporal changes in groundwater contamination and in land use across a vast spatial extent encompassing natural environments, agricultural regions, and urban areas. This effort will enable breakthrough advances to improve the mapping of hazardous areas with different levels of vulnerability, and to assess the efficacy of land use planning toward groundwater protection.

In this context, this study focuses on advancing the use of statistical methods to assess groundwater vulnerability by explicitly introducing the time dimension in the analysis. The objectives are to address recent requirements from transnational policies and to close the critical information gap described earlier.

In view of current and projected acceleration in global urbanization, urban areas are widely considered as one of the most important non-point sources of contamination impacting groundwater quality (Kuroda and Fukushi 2008). The European Environment Agency (2006) reported that the expansion of urban areas in many eastern and western European countries has increased by over three times the growth of population between 1986 and 2006 (EEA 2006). Urban sprawl is one of the most important types of land-use changes impacting the regional environment, the social structure, and the economy in Europe. Urban sprawl generally follows periods of rapid urbanization associated with population growth and with the excessive migration of people from rural to urban areas. The Po Plain in northern Italy is one of the most populated regions in Europe with a similar pattern: an initial phase of urban area expansion from the 1950s to the 1970s followed by an urban sprawl in the subsequent decades. This pattern qualifies the Po Plain as

a representative “pilot area” to identify the interplay of urbanization and environmental, social and economic impacts after the rapid urban increase.

Nitrate is an abundant contaminant of groundwater. With a high mobility and multiple sources, nitrate is an effective indicator of groundwater contamination. A sufficient frequency for monitoring nitrate concentration in groundwater over the long term allows the use of nitrate in temporal analyses to determine the contamination trend.

Recent studies (Masetti et al. 2008, 2009; Sorichetta et al. 2011) have shown that, in some areas of the Po Plain, nitrate occurrence in groundwater is strongly related to urban sources (using population density as a proxy) more than to agricultural activities; however, the problem has never been analyzed in the time dimension. It is unclear whether a relationship exists between recent changes in groundwater nitrate contamination and in land use. To analyze how urban development could affect groundwater quality in the 2000s, recent trends in groundwater nitrate concentration need to be correlated with the evolution of potential urban nitrate sources across this region.

While satellite data have been typically used to qualitatively assess the availability of groundwater resources (Jha and Chowdary 2007; Tweed et al. 2007; Al Saud 2010; Jha et al. 2010; Jasmin and Mallikarjuna 2011; Frappart et al. 2011; Wang et al. 2014), only a limited number of studies used satellite data to quantitatively assess groundwater quality (Werz and Hötzl 2007). The use of an innovative dataset to delineate urban areas with satellite scatterometer data has been explored to identify zones where different rates of urban growth occurred across the entire study area, and in which an increase of potential urban sources may exist and consequently impact groundwater. Radar backscatter data acquired by the SeaWinds scatterometer aboard the QuikSCAT satellite together with the Dense Sampling Method (QSCAT-DSM; Nghiem et al. 2009) have been used to identify and map urban extent and surface features at a posting scale of about 1 km². QSCAT-DSM results are to be compared with those obtained from two different sources of urban information: (1) changes of population density and (2) changes in land use derived from high-resolution aerial images acquired in different years.

In addition, to address the time dimension in groundwater vulnerability assessment, this study can be considered to be the first to use remote sensing data to obtain a quantitative assessment of groundwater quality changes through time. Moreover, it also represents one of the first applications of QuikSCAT data to environmental and hydrogeological problems with an optimal spatial scale enabled by DSM.

In this study, a “zone vulnerable to nitrate contamination” can be defined as an area where the combination of natural (e.g., groundwater depth and velocity) and anthropogenic factors (e.g., growth of urban areas) involves a deterioration trend of groundwater quality. In a static system, a “zone vulnerable to nitrate contamination” can be defined as an area where the combination of

the same factors involves a given absolute level of contamination in the aquifer.

Study area

The study area is located within the Po Plain area of Lombardy region, and covers an area of 13,400 km², where urban, industrial, livestock and agricultural activities are extensively and heterogeneously present.

This region is surrounded by important rivers influencing groundwater flow in the unconfined aquifer: Po River along the south; Ticino, Sesia and Po rivers along the west; and Mincio River along the east (Fig. 1). It is also constrained by mountain chains forming the boundary of the plain: Lombardy Prealps along the north and Appennines along the southwest.

This area has a complex hydrogeological setting consisting of multiple aquifers with various properties and interactions. The Lombardy plain subsoil is characterized by Plio-Pleistocene sediments whose upper unit forms the shallow unconfined aquifers (Fig. 2). Sediments are mainly gravels and sands, although the presence of finer sediments increases from the north to the south where shallow aquifers are mainly constituted by fine sands and are partially confined. These aquifers have high transmissivity, ranging

from 10⁻² to 10⁻⁴ m²/s and medium-high hydraulic conductivity, ranging from 10⁻⁴ to 10⁻⁶ m/s, while its thickness ranges from 40 to 80 m (Regione Lombardia and ENI 2001).

The groundwater flow is generally oriented north-south toward the base level defined by the Po River, with a deviation to east-south-east in the south-east area of Lombardy. The groundwater depth decreases from north to south, ranging from values higher than 70 m to less than 2 m. There are also some groundwater-fed streams, where the local groundwater depth reduces to zero.

Nitrate (NO₃⁻) is the most common non-point-source contaminant found in groundwater in the Po Plain. Nitrate concentrations have been monitored by a network of about 500 wells covering the entire area with a nearly uniform spatial distribution, where data have been collected every 6 months from 2001 to 2011 (Regional Environmental Agency – ARPA, unpublished data, 2012). From the network, only the 221 wells monitoring the shallow aquifer and having a minimum of eight measurements were selected for being used in the analysis. As an example (Fig. 1), two photographs taken during the PO PLain EXperiment (POPLEX) in May 2014 (Masetti et al. 2014; Nghiem et al. 2014a) show rural and urban areas as two major contrastive types of land use where the monitoring wells are located.

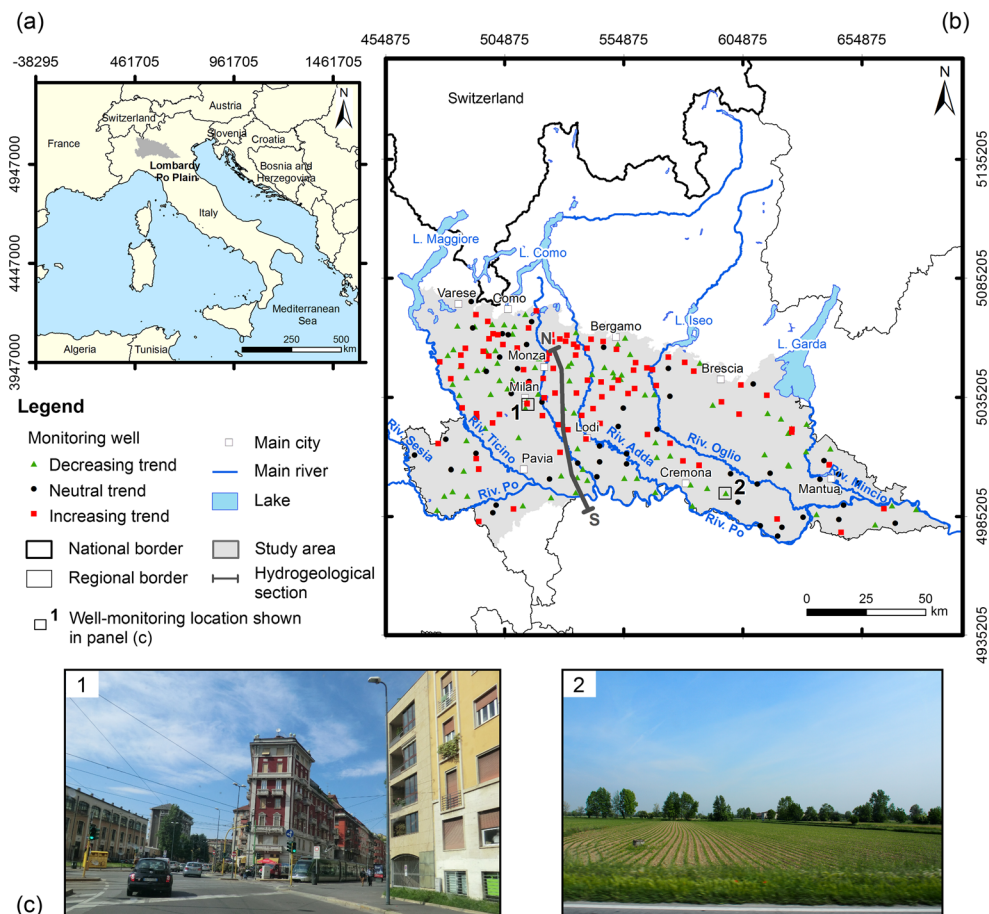


Fig. 1 a Location of the study area; b well-monitoring network; c examples of well locations in urban (1) and rural (2) environments as marked by 1 and 2 next to the square boxes on the map (b) where the photographs were taken during the POPLEX field campaign in May 2014. Coordinates refer to WGS 1984 – UTM Zone 32 N projection

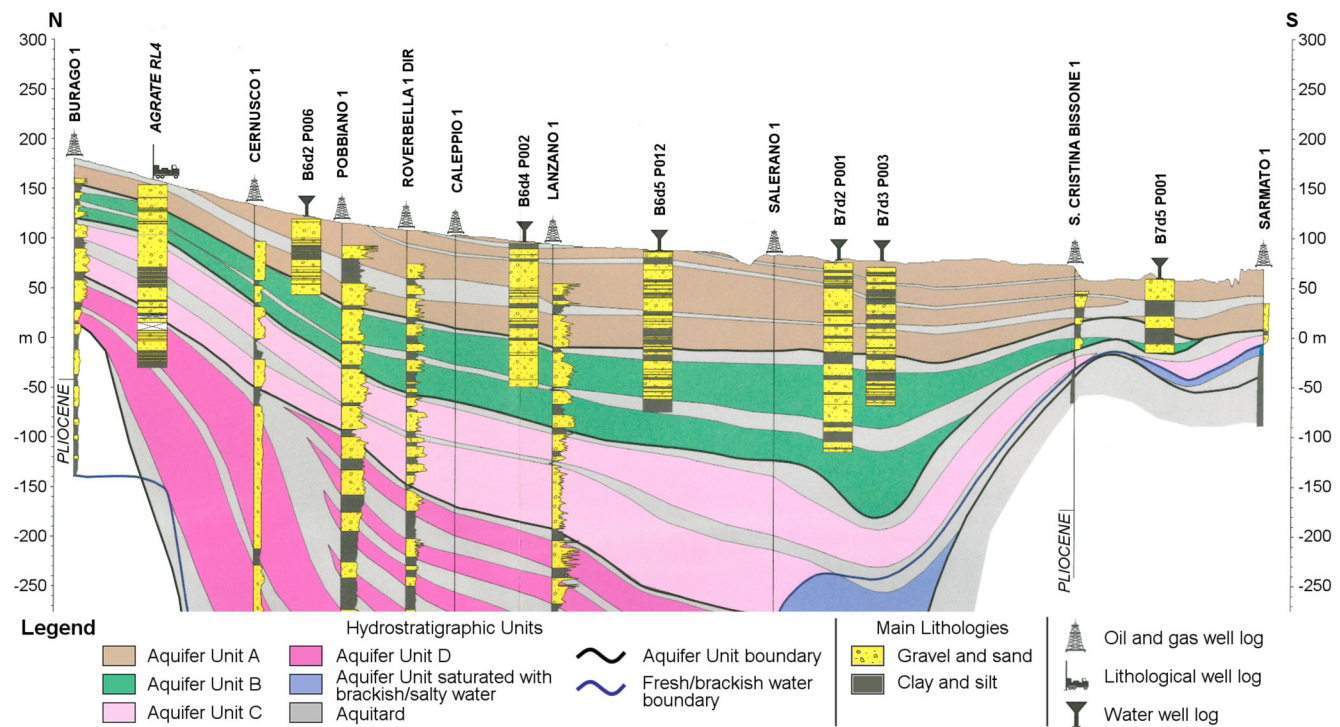


Fig. 2 Hydrogeological scheme along the N–S section marked by the grey line on the map in Fig. 1b (modified from Regione Lombardia and ENI 2001)

This study focuses on the evolution of nitrate concentration in groundwater related to changes of urban areas. The change in nitrate concentration is quantified by the slope of the regression line from an interpolation of concentration data. The slope defines the rate of nitrate concentration change in mg/L per day. Positive slope values show increasing concentration trends representing water quality deterioration, while non-positive slope values indicate steady or decreasing concentration trend characterizing unaffected or improved groundwater quality.

Until the end of the considered monitoring period in 2011, about 28 % of wells show increasing concentration trends and concentrations exceeding the guideline value of 25 mg/L defined by the EU standard (91/676/EEC; European Community 1991), while 35 % of wells show decreasing concentration trends and concentrations lower than the same guideline value. Only 3 % of wells show increasing concentration trends and concentrations exceeding the established threshold of 50 mg/L (91/676/EEC, European Community 1991; 2006/118/EC, European Community 2006; Table 1). Wells with concentrations higher than the guideline value of 25 mg/L are located mainly in the northern sector, while those with concentrations lower than the guideline value are mostly located in the southern sector.

Method and materials

Method

The weights of evidence (WofE) modeling technique combines different spatial datasets in a geographical information system (GIS) environment to analyze and

describe their interactions and generate predictive patterns (Bonham-Carter 1994; Raines et al. 2000). WofE can be defined as a data-driven Bayesian method in a log-linear form that uses known occurrences representing the response variable as training sites (training points). These data are used to obtain predictive probability maps (response themes; i.e., groundwater vulnerability maps) from multiple weighted evidences (i.e., evidential themes representing explanatory variables or factors that influence groundwater vulnerability), which determine the spatial distribution of the occurrences in the study area (Raines 1999). Training points (TPs) are used in WofE to calculate the prior probability, the weights for each class representing a different range of values of each generalized evidential theme, and the posterior probability values in the response theme.

Prior probability is based on prior knowledge of the TPs' locations in the study area. Prior probability is simply defined by the ratio between the area containing occurrences (i.e., the number of pixels containing a training point D) and the total area (i.e., the total number of pixels). Thus, the prior probability represents the probability that a pixel within the study area contains an occurrence without considering any evidential themes, and it can be expressed as (Bonham-Carter 1994):

$$P\{D\} = \frac{N_D}{N_T} \quad (1)$$

where N_D and N_T are respectively the number of pixels containing a training point and the total number of pixels in the study area.

Table 1 Nitrate concentration trends related to the last measured concentration (percentage of wells)

	Increasing concentration trend	Decreasing concentration trend
Concentration ≥ 25 mg/L in 2011	28 %	18 %
Concentration < 25 mg/L in 2011	19 %	35 %
Concentration ≥ 50 mg/L in 2011	3 %	6 %
Concentration < 50 mg/L in 2011	44 %	47 %

For each class of each evidential theme, a positive and a negative weight are computed based on the location of the TPs with respect to the study area. For a given class B , the positive weight W^+ and the negative weight W^- are, respectively, higher and lower than zero or lower and higher than zero. The resulting combination depends on whether B has more or fewer TPs than expected by chance.

The weights can be expressed as (Bonham-Carter 1994):

$$W^+ = \log_e \frac{P\{B|D\}}{P\{B|\bar{D}\}} \quad (2)$$

$$W^- = \log_e \frac{P\{\bar{B}|D\}}{P\{\bar{B}|\bar{D}\}} \quad (3)$$

where $P\{B|D\}$ and $P\{B|\bar{D}\}$ are respectively the probability of a pixel being in class B when the same pixel contains or does not contain a training point, and $P\{\bar{B}|D\}$ and $P\{\bar{B}|\bar{D}\}$ are respectively the probability of a pixel not being in class B when it contains or does not contain a training point.

The contrast (positive weight minus negative weight) represents the overall degree of spatial association between each class of a given evidential theme and TPs. Thus, it is a measure of the usefulness of the considered class in predicting the location of TPs (Raines 1999). A confidence value for the ratio between the contrast and its standard deviation must be selected to provide a useful measure of the significance of the contrast (Raines 1999). For this study, a confidence value of 1.282, corresponding approximately to a 90 % level of significance, was chosen as the minimum acceptable value for considering an evidential theme class as statistically significant.

The posterior probability represents the relative probability that a pixel contains an occurrence based on the evidences provided by the evidential themes (i.e., based

on the calculated weights). The posterior probability can be expressed as (Bonham-Carter 1994):

$$\log_e O\{D|B_1^k \cap B_2^k \cap B_3^k \dots \cap B_n^k\} = \sum_{j=1}^n W_j^k + \log_e O\{D\} \quad (4)$$

where n identifies each single class used to categorize each evidential theme, k is either + or - depending on whether the prediction spatial class, B_n , is either present or absent, and $O\{D\}$ is the odd form of the probability that a pixel within the study area contains an occurrence.

The relative probability means that a pixel having a higher posterior probability is more likely to contain an occurrence than a pixel having a lower probability, and it represents a measure of the relative likelihood of occurrence of an event (Raines 1999). In this study, the WofE response themes were generated using the Spatial Data Modeler (Sawatzky et al. 2009) for ArcGIS 9.3 (ESRI 2008).

Response variable

For the purpose of this study, the response variable is represented by nitrate concentration trend in groundwater. The WofE modelling technique requires a binary formulation of the response variable.

A frequency histogram of nitrate concentration trend shows a nearly bimodal distribution with two main relative peaks at about -0.0008 and $+0.00016$ mg/L per day (Fig. 3). Another minor peak can also be identified at value 0. The intermediate values of -0.0004 and $+0.0004$ mg/L per day, which separate three populations, were considered to be appropriate values to be used as thresholds.

Wells showing concentration trends higher than $+0.0004$ mg/L per day are considered as “increasing” wells (87), and those below -0.0004 mg/L per day as “decreasing” wells (86). Wells showing concentration trends included in the range -0.0004 and $+0.0004$ mg/L per day are considered as “neutral” wells (48). In these wells, the uncertainty in the slope coefficient value, which is close to zero, does not allow one to precisely categorize them as “increasing” or “decreasing” wells. The “increasing” wells, showing a clear increase in concentration trends, represent the training set, and they have been selected to be used in the analysis. While “decreasing” and “neutral” wells are grouped in a unique set, representing the control set.

Evidential themes

Both natural and anthropogenic factors have been used as evidential themes in the analysis. Natural factors include geological and hydrogeological conditions of the study area and are considered static for the purpose of the study. Three different factors have been selected to represent changes of urban nitrate sources through time, i.e. land

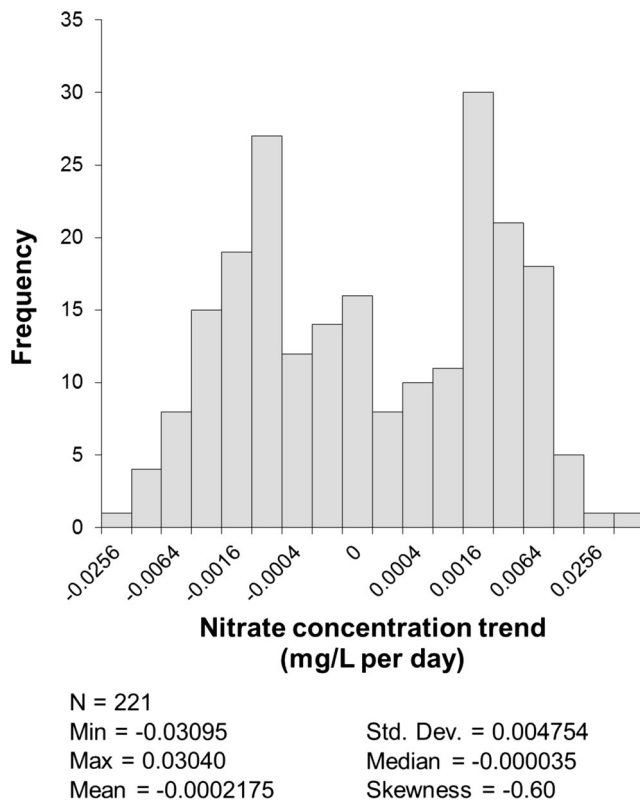


Fig. 3 Frequency histogram of nitrate concentration trend

use change derived from (1) satellite data, (2) aerial photographs, and (3) data on population density changes. Details on each of the factors and on how they are used in the study are presented in the following.

Urban nitrate sources: anthropogenic factors

Nitrogen loading derived from urban areas (presence of sewer leakage or septic tanks) cannot be easily or directly estimated quantitatively. For this reason, it is necessary to explore other variables that can be used as a proxy.

For this purpose, it is crucial to have a temporally and spatially consistent dataset delineating the urban area extent through time in order to investigate the potential relationships between its variation and the evolution of groundwater contamination. Even in the data-rich European and North American countries, such information is not collected consistently or during consistent periods of time and is often spatially and/or temporally limited.

Population density has been used often as a proxy for urban nitrate sources in groundwater vulnerability assessments (Nolan 2001; Nolan et al. 2002; Masetti et al. 2009; Sorichetta et al. 2011). Population density is generally referred to administrative units at the specific time of the demographic census or survey. Official national censuses are usually done once every 10 years. Consequently, analyses based on population census cover a period of 10 years, missing changes in shorter periods.

In this study, the population-density change is calculated as the difference between population densities in

each district referred to two successive national censuses, in 2001 and 2011 (ISTAT 2001, 2011). Positive values indicate a growth of population, and negative values represent a reduction of population. Between 2001 and 2011, population density changed in the range of -402 to $+845$ people/km² across Lombardy (Fig. 4).

High-resolution aerial images in Lombardy have been periodically acquired by the Agency of Services of Agriculture and Forest (ERSAF), creating a database called DUSAF (ERSAF 2014), to identify and categorize the land cover in five main land use classes: urban areas, agricultural areas, woods and semi-natural environments, wetlands and surface-water areas. The technical maps are at a 1:10,000 scale. For the purpose of the study, vector maps have been transformed to raster format. DUSAF is updated at irregular intervals that can be different for different sectors of the region. This limitation does not allow the maps to represent the urban land use at the same time across the whole region.

To observe changes in urban extent, the two relevant groups are: urban areas, and non-urban areas consisting of the remaining four classes in DUSAF. Urban-extent changes are calculated as the percentage change of urban areas in each 1 km² pixel, between two successive compilations, in 2000 (DUSAF version 1.1) and in 2007/2009 (DUSAF versions 2.1 and 3.0), depending on the last available data in different sectors of the study area. Positive values indicate an expansion of urban areas, while negative values indicate a reduction of urban areas. According to DUSAF data, urban-area extent changed in the range of -6.7 to $+30.8$ % (Fig. 5).

Radar satellite remote sensing data can be used to identify and delineate urban areas. In fact, satellite radar backscatter is dependent on the number, density, size and material of buildings (e.g., higher backscatter for more buildings, for larger and taller buildings, and for stronger materials like steel rather than wood). Crucially, the satellite global coverage with regular data acquisitions in time spanning over a decadal period allows continuous monitoring of urban changes, and thus enables the trend analysis together with changes in nitrate sources, capturing more detailed variability in annual, interannual, and decadal time scales. Such a satellite dataset has been collected by the SeaWinds scatterometer aboard the QuikSCAT satellite (QSCAT) in the decade of the 2000s. QSCAT backscatter measurement is accurate to 0.2 dB ($3\text{-}\sigma$; Nghiem et al. 2004), which is equivalent to approximately 1.57 % in root-mean-square error, enabling QSCAT to detect not only large and rapid changes as well as small and slow variations. Applied on the original QSCAT backscatter data, the dense sampling method (DSM), based on a newly invented mathematical transform called Rosette Transform (Nghiem et al. 2009), is a breakthrough enabling quantitative measurements of urban parameters (i.e., location, shape, extent, and typology) to map land cover features at a posting pixel scale of 1 km², and to calculate the rate of urban change in the decadal period of 2000–2009 in every pixel across the world.

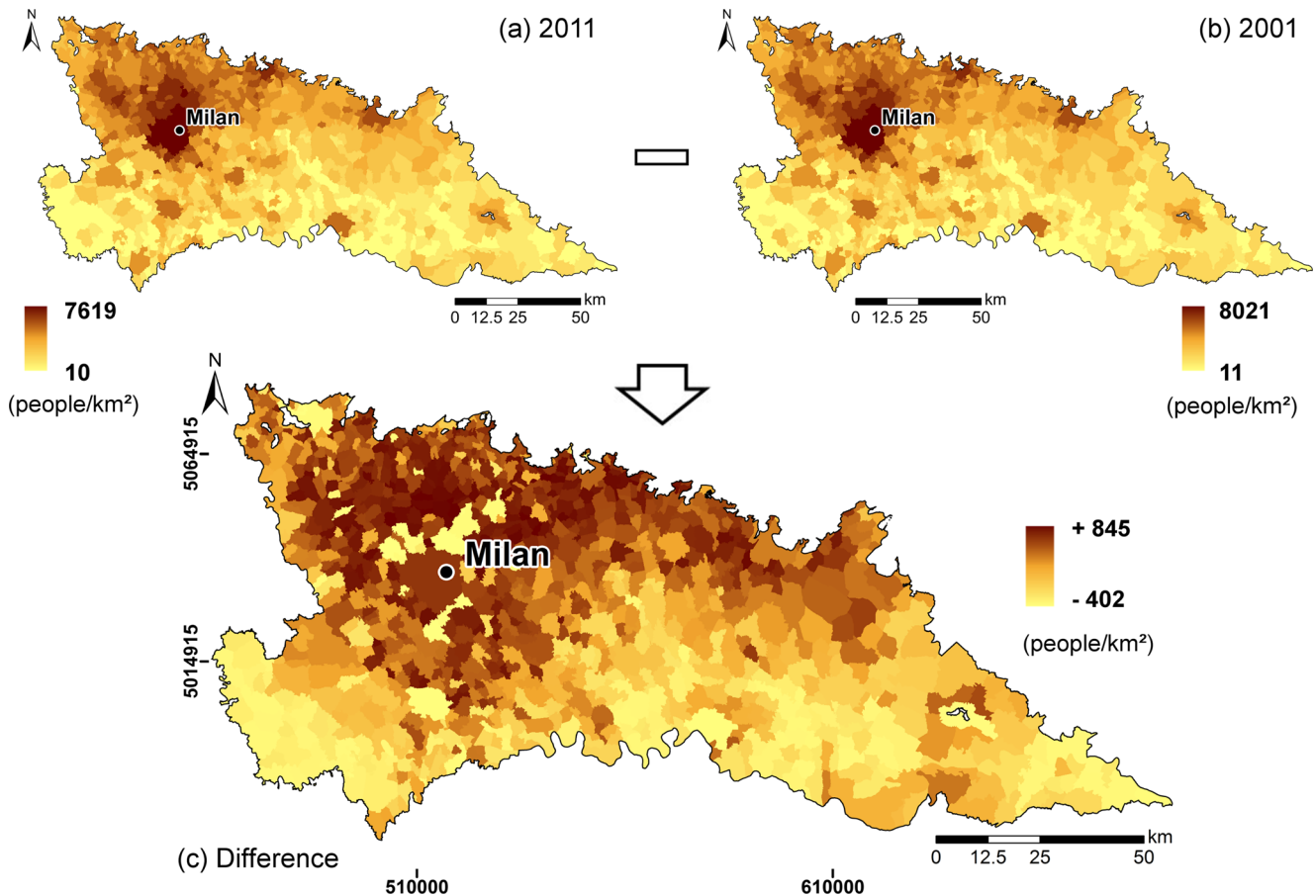


Fig. 4 Population density maps, at municipality level, in **a** 2011 and **b** 2001, and **c** the final map obtained as the difference between the two maps (**a–b**). Coordinates refer to WGS 1984 – UTM Zone 32 N projection

In DSM, backscatter signature of an area is characterized by the composition of a spatially dependent mean part and a fluctuation part that is a function of location, azimuth angle (buildings are different on different sides; roads have preferential directions; hilly surfaces in a city, etc.), and any changes in time (vehicles and people move in a city; there can be rain, snow, hail, etc. at different times in different sections of a city). Thereby, DSM allows azimuthal and temporal changes to occur, and high-resolution results from DSM include information from both the mean value and the variability of backscatter at each location where the Rosette Transform is applied on an ensemble of backscatter data whose centroids are collocated in each unit area. At the expense of the daily temporal resolution, DSM is a breakthrough method to increase the spatial resolution in urban areas, where the inherent azimuth and motion changes invalidate the use of the traditional deconvolution method to enhance the resolution of satellite remote sensing data.

Moreover, advantages of QSCAT-DSM (Nghiem et al. 2009) include the delineation of urban and suburban contours both in metropolitan and rural areas, and the identification of urban development both fast and expansive or slow and restrained. Some limitations are due to complex mountainous topography, persistent snow cover on cold land at high latitudes (e.g., tundra

and taiga), or extensive water surfaces, which affect backscatter signatures, but such factors are ineffective in the study area. The pointing accuracy of DSM was verified precisely with an accurate overlay of the Príncipe Island (Gulf of Guinea) on its true geographic location (Nghiem et al. 2009). DSM was validated and used to accurately delineate urban extent for a number of cities in different countries such as Dallas-Fort Worth and Phoenix in the United States, Bogotá in Colombia, Dhaka in Bangladesh, Guangzhou and Beijing in China, and Quito in Ecuador (Nghiem et al. 2009; Nghiem et al. 2014b).

The rate of land cover change, including both urban and rural areas, is determined by the slope of the linear regression with QSCAT-DSM data obtained for each year in 2000–2009, expressed in decibel per year (dB/year). Positive slope values represent increasing or growth of urban areas, while non-positive and shallow slope values indicate steady rural areas or natural environments. QSCAT-DSM slope varies within the range of -0.0699 to $+0.1268$ dB/year, or equivalently -16.0 to $+29.6$ %/decade (Fig. 6), as the slope in dB/year can be converted to the 10-year percentage change given by $100 \times (10^{\text{dB/year}/10} - 1)$.

In this study's approach to assess impacts on groundwater contamination, the focal method is adapted particularly for

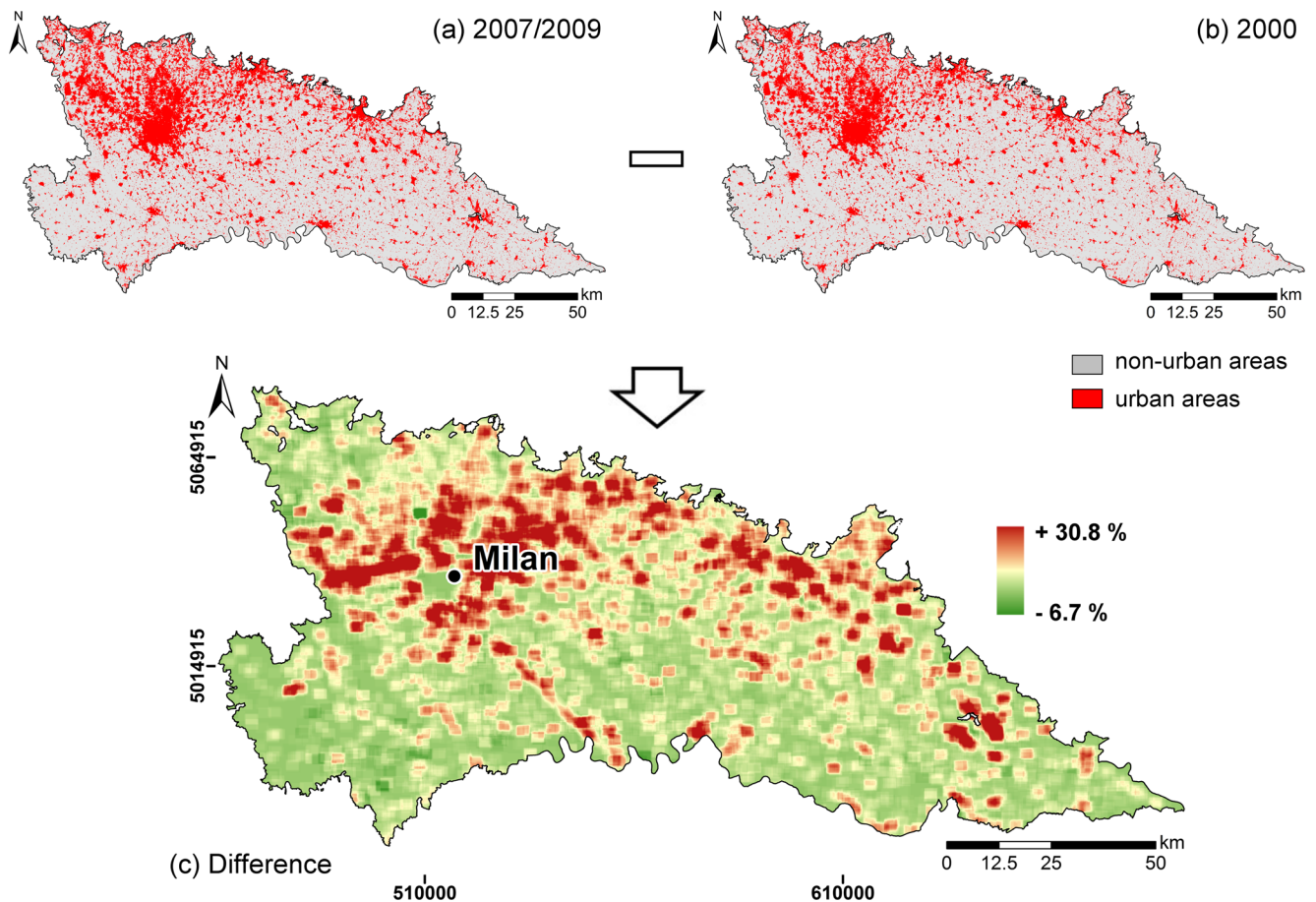


Fig. 5 DUSAF urban area extent maps in **a** 2007/2009 and **b** 2000, and **c** the final map obtained by calculating the percentage change of urban areas between the two maps (**a–b**) at a resolution of 1 km^2 . Coordinates refer to WGS 1984 – UTM Zone 32 N projection

applications to QSCAT-DSM and hydrogeological data, and to DUSAF as well. The algorithm in the focal method considers both the value of each cell and the values of the surrounding cells with a deterministic mathematic function. It can account for groundwater flow direction: among the surrounding cells of each cell, only the cells located upstream are considered in the calculation. The extent of the area of calculation is 9 km^2 for a 3×3 window above each pixel of 1 km^2 .

Urban nitrate sources: natural factors

Natural factors, characterizing geological and hydrogeological conditions of the study area, are considered to be static in this study. While groundwater depth has a seasonal variability, it has not significantly changed over the Po Plain in the decade 2000–2009.

Soil protective capacity is obtained from existing data (Fig. 7a). It was produced by the Agency of Services of Agriculture and Forest. This soil variable has been mapped at a 1:250,000 scale to assign soil to three protective capacity classes: high, moderate and low. The variable describes soil capacity to reduce water-soluble polluting substances leaching from the surface. It is related to filtering and buffering capacity because of both

mechanical and biological/microbiological activities contributing to degradation (Masetti et al. 2007).

The following describes the other three hydrogeological variables, characterizing the shallow unconfined aquifer, that were obtained for this study. Groundwater depth was derived from the difference between the topographic level and groundwater piezometric levels (regional survey in 2003; Fig. 7b). The groundwater depth decreases from north to south, ranging from values higher than 70 m to less than 2 m. At some local areas, there are groundwater-fed streams where groundwater depth is reduced to zero.

Groundwater velocity was estimated from 1,263 wells where pumping tests were available to determine hydraulic conductivity (Fig. 7c). These values were used together with the local hydraulic gradient to obtain groundwater velocity. Field data were interpolated through the kriging methodology to obtain a map of the distribution of groundwater velocity. In the study area, groundwater velocity ranges from 4.7×10^{-8} to 7.3×10^{-5} m/s. Higher values are located in the northern sector and in some areas of the southwestern sector, while lower values are mainly found in the southeastern sector.

Hydraulic conductivity of the vadose zone was determined from 1,597 well stratigraphy records (Fig. 7d).

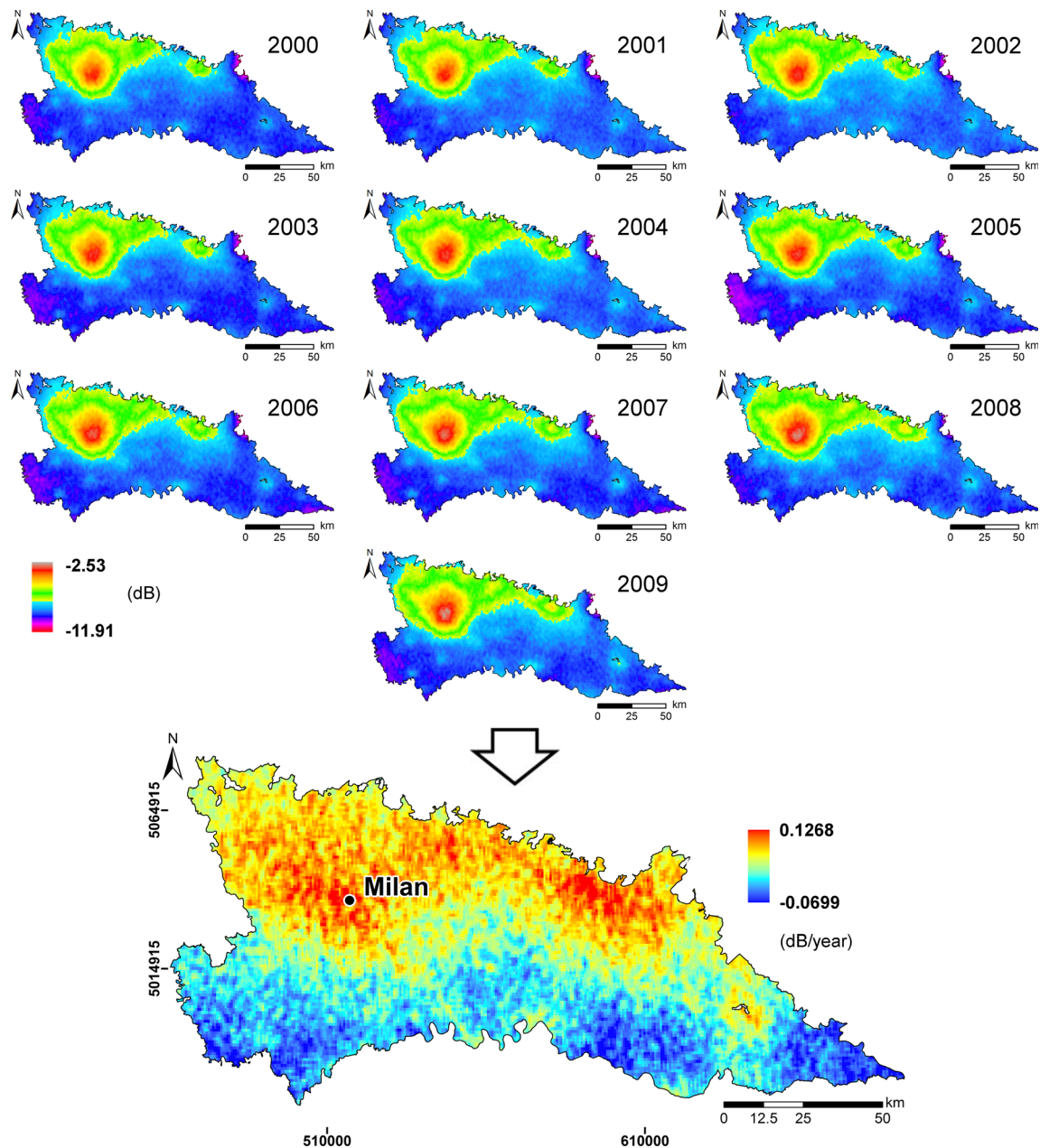


Fig. 6 QSCAT-DSM backscatter maps, at a posting of 1 km^2 , from 2000 to 2009, and the final map of the linear regression slope. Coordinates refer to WGS 1984 – UTM Zone 32 N projection

For each well, the hydraulic conductivity was calculated with the equivalent vertical permeability method (Anderson and Woessner 1992), considering the thickness of the layers in the vadose zone in the calculation of the hydraulic conductivity. Data were then interpolated through kriging methodology to obtain the map of the distribution of hydraulic conductivity of the vadose zone in the study area. Hydraulic conductivity of the vadose zone ranges from 4.1×10^{-8} to 4.0×10^{-2} m/s. Higher values are located in the northern sector, especially along the belt of the heads of groundwater-fed streams and along the main rivers (Ticino and Adda rivers).

Results and discussion

Impacts observed from the independent variables

The contrasts of statistically significant evidential themes enable an assessment of the influence of the variables under consideration on groundwater contamination. Contrast values, both for anthropogenic and natural factors, are presented in Fig. 8. All three variables, representing urban nitrate sources and their evolution, show a positive correlation between the increase of urban areas or population growth and the occurrence of increasing nitrate concentration trends in groundwater.

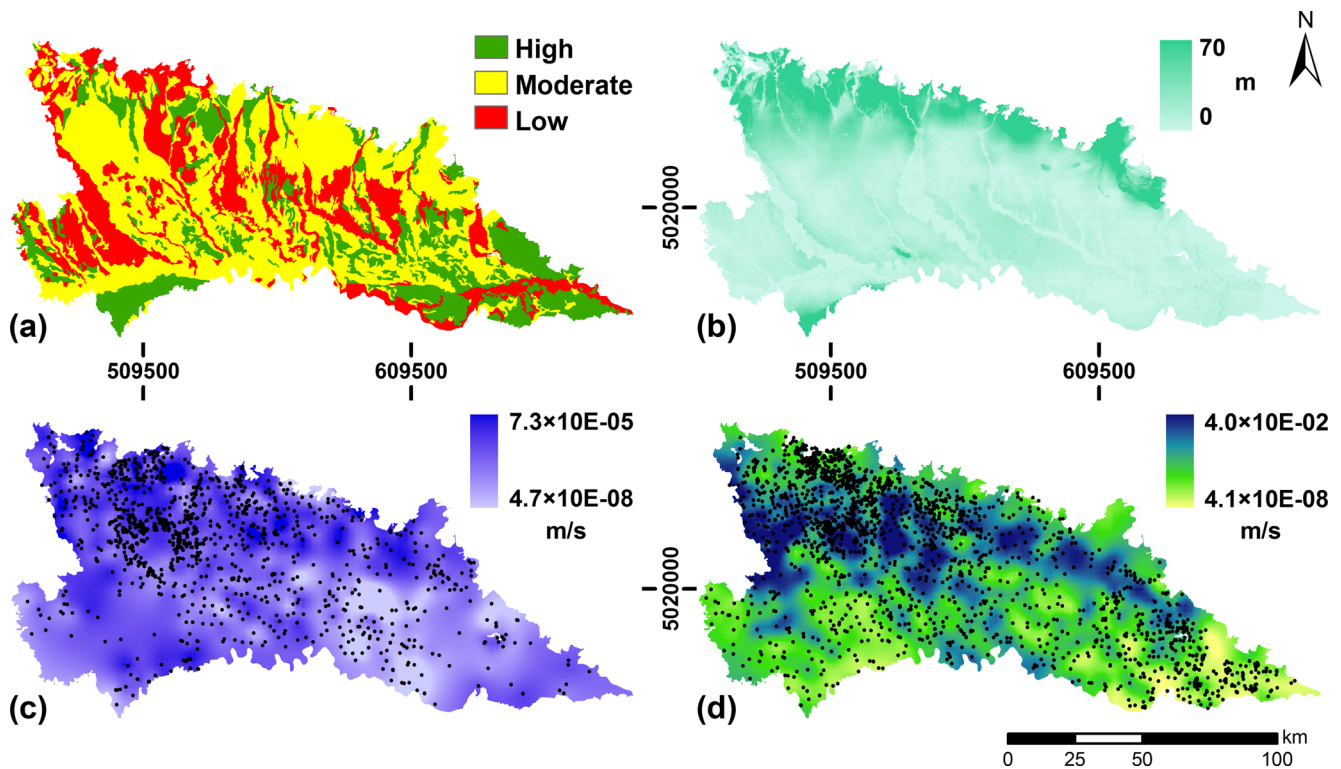


Fig. 7 Natural factors maps: **a** soil protective capacity; **b** groundwater depth; **c** groundwater velocity; **d** hydraulic conductivity of the vadose zone. **c–d** Dots represent the locations of pumping test sites and well stratigraphies used to map the spatial distribution of groundwater velocity and hydraulic conductivity of the vadose zone, respectively. Coordinates refer to WGS 1984 – UTM Zone 32 N projection

Threshold values, corresponding to the transition from negative to positive contrasts, are $+44$ people/km², $+0.0260$ dB/year and $+1.81$ % over the study period, respectively for population density change, QSCAT-DSM slope and DUSAF urban extent change. Observed from these variables, classes with positive contrasts are clustered in the northern sector, while classes with negative contrasts are mainly in the southern sector.

Soil protective capacity is not statistically significant. Also, it does not show a discernible correlation, with negative contrasts for low and high classes and a positive contrast for moderate classes. Groundwater depth reveals that large values of water-table depth are positively related to increasing concentration trends, while low values (close to surface or less than 13 m) are negatively associated. Groundwater velocity and hydraulic conductivity of the vadose zone show positive correlations and the threshold values are about 1.5×10^{-6} m/s and 4.7×10^{-6} m/s, respectively.

Response themes and vulnerability maps

In order to evaluate the reliability of each variable as a proxy of urban nitrate sources, three response themes were obtained and compared (Fig. 9). Each response theme considers one of the three urban variables, and the three statistically significant evidential themes represent the associated natural factors (Table 2).

Each response theme was categorized so that each vulnerability class in the corresponding map contains approximately the same number of different posterior probability values according to the geometric interval method (Sorichetta et al. 2011). Five classes were identified with the degree of groundwater vulnerability increasing from 1 to 5. This number was selected based on the general criteria used to identify vulnerability classes (Sorichetta et al. 2011) and on visual analytic techniques (Cowan 2001).

It is important to note that these response themes are time dependent. This means that groundwater vulnerability classes reflect the tendency toward a deterioration of the quality of the aquifer rather than the absolute severity of the aquifer contamination in a static condition.

Reliability and validation of the maps

The general quality of each response theme (i.e., post probability map) can be evaluated with the area-under-the-curve (AUC) value. AUC is a direct measure of the performance of the statistical approach, and is given by the area under the curve (integral) for cumulated area/cumulated training points expressed in percentage. The calculated AUC values are presented in Table 2 showing the consistent quality of the different maps.

Then, the reliability of each classified map was evaluated again by considering its overall performance in classifying the occurrences. Two statistical validation

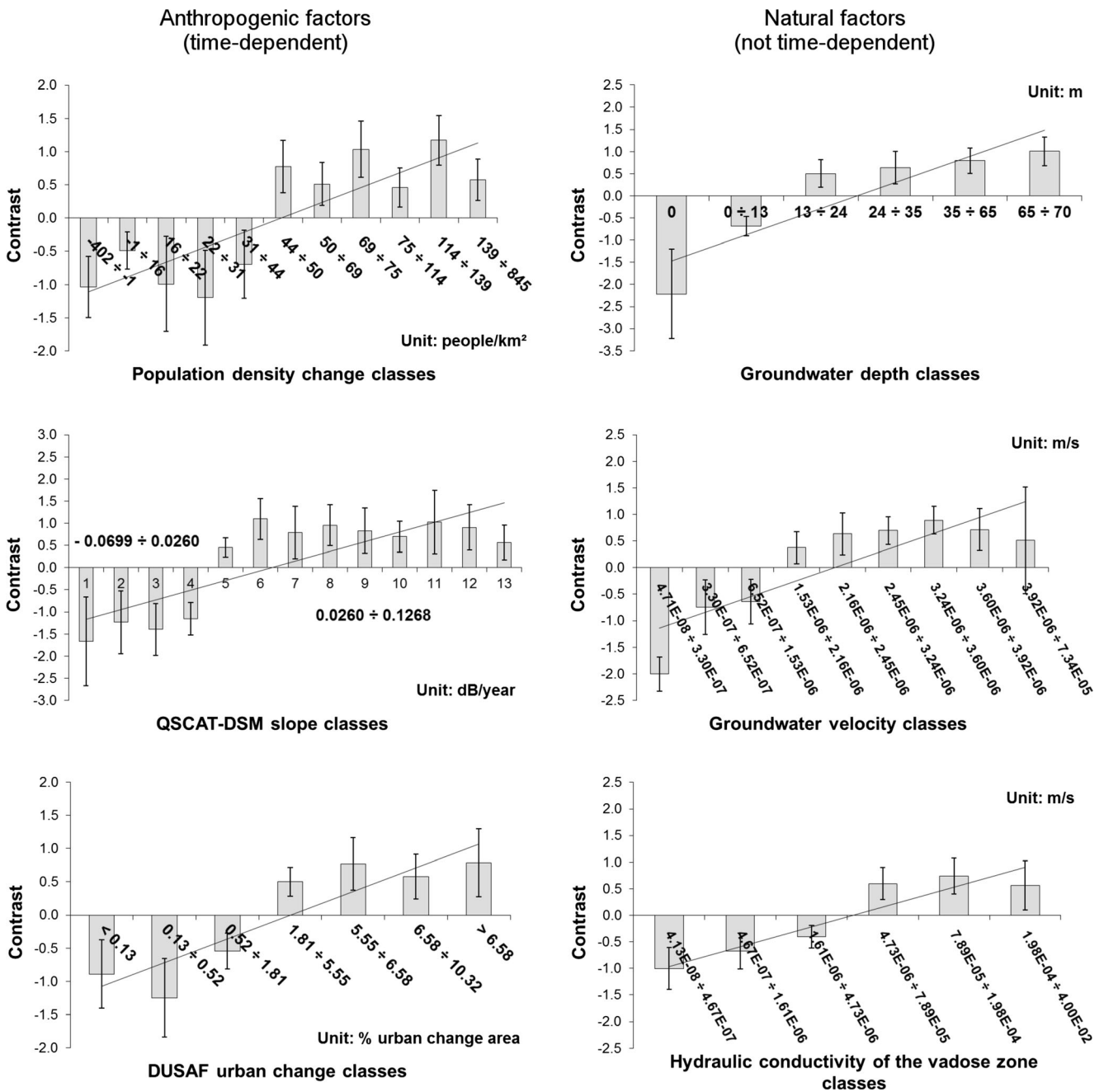


Fig. 8 Contrasts and error bars of the statistically significant classes of each evidential theme used to generate the maps in Fig. 9

procedures were used: (1) frequency of training set, and (2) average nitrate concentration trend of all wells in each vulnerability class.

The evaluation of the frequency, F , is expressed by the ratio:

$$F = (N_{Wj} / T_{Wj}) \tag{5}$$

where N_{Wj} is the number of “increasing” wells in a vulnerability class j and T_{Wj} is the total number of wells in the same class j . This technique adds new information to the validation process because it also includes the wells not used in the modeling. Frequency is expected to increase monotonically as the degree of vulnerability increases. The expected trend is verified. In fact, for all the three vulnerability maps, there are no

“increasing” wells in the lowest vulnerability class and the highest frequency of “increasing” wells is in the highest vulnerability class (Fig. 10).

The evaluation of the average nitrate concentration trend of all wells, C_{AVG} , is expressed as:

$$C_{AVG} = \frac{\sum_{i=1}^{T_{Wj}} C_{ij}}{T_{Wj}} \tag{6}$$

where C_{ij} is the nitrate concentration trend of well i in the vulnerability class j , and T_{Wj} is the total number of wells in the same class j . This analysis was carried out using all wells stored in the database. The concentration should

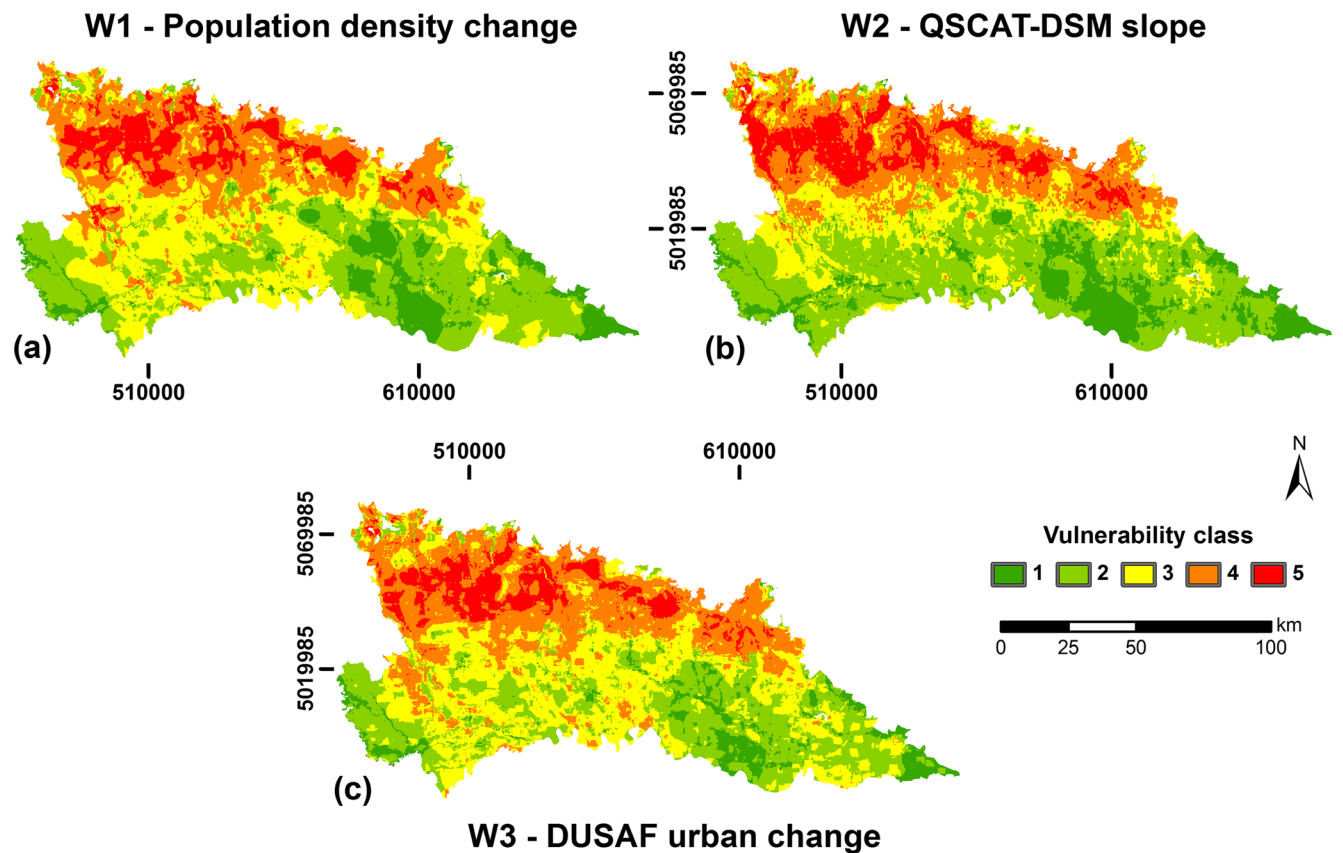


Fig. 9 Vulnerability maps obtained using static variables, representing natural factors, with **a** population density change, **b** QSCAT-DSM slope, and **c** DUSAF-based urban extent change as time-dependent variables. Coordinates refer to WGS 1984 – UTM Zone 32 N projection

monotonically increase as the degree of vulnerability increases and the central vulnerability class should give a value close to the overall mean value. Despite some anomalies, all three histograms show a direct correlation between average nitrate concentration trend and the degree of vulnerability (Fig. 10). With these two techniques, the quality of each vulnerability map was evaluated based on the slope coefficient of the regression line and the regression coefficient, so that a map should be deemed reliable if it passes these tests.

Spatial agreement between maps

A spatial agreement is quantitatively evaluated through a pixel-by-pixel analysis representing the difference, expressed as percentage, in the unit-cell classification for

Table 2 Combination of evidential themes used to obtain response themes and AUC values (*pop* population density change, *gwd* groundwater depth, *gww* groundwater velocity, *hcv* hydraulic conductivity of the vadose zone, *QSCAT-DSM* land use changes derived from satellite data, *DUSAF* land use changes derived from aerial photographs)

Response theme	Combination of evidential themes	AUC value theme
W1	pop, gwd, gww, hcv	74.4 %
W2	QSCAT-DSM, gwd, gww, hcv	74.3 %
W3	DUSAF, gwd, gww, hcv	73.7 %

the three vulnerability maps (Fig. 11). Results from this analysis show a high level of agreement between the maps in the paired map-to-map comparison: almost 61–67 % of the study area is classified with the same degree of vulnerability, 33–38 % is classified within a difference of one degree of vulnerability, while only 0.3–0.8 % are within a difference of two degrees of vulnerability.

Another method to evaluate the reliability of each vulnerability map is overlaying each map with the classes of its urban change variable with positive contrast values to examine their consistency (Fig. 12). Map W2, obtained using QSCAT-DSM slope, is the only one where the highest vulnerability classes are consistently overlain by the classes of urban extent change variable with positive contrast values. Instead, in the other two cases there are anomalous mismatches. In map W1, obtained using population density changes, some cities (like Monza or Brescia) show negative contrast values, meaning that their population density change is lower than +44 people/km². In map W3, obtained using DUSAF maps, some areas in the northern sector show negative contrast values (like Milan), while agricultural areas of the southern sector are characterized by positive contrast values (e.g., Provinces of Cremona and Mantua). The first anomaly could be explained by the urban sprawl phenomenon, with residential citizens moving from the largest cities to the smallest cities, while the rate of urbanization is increasing almost everywhere. The second anomaly could be caused by the

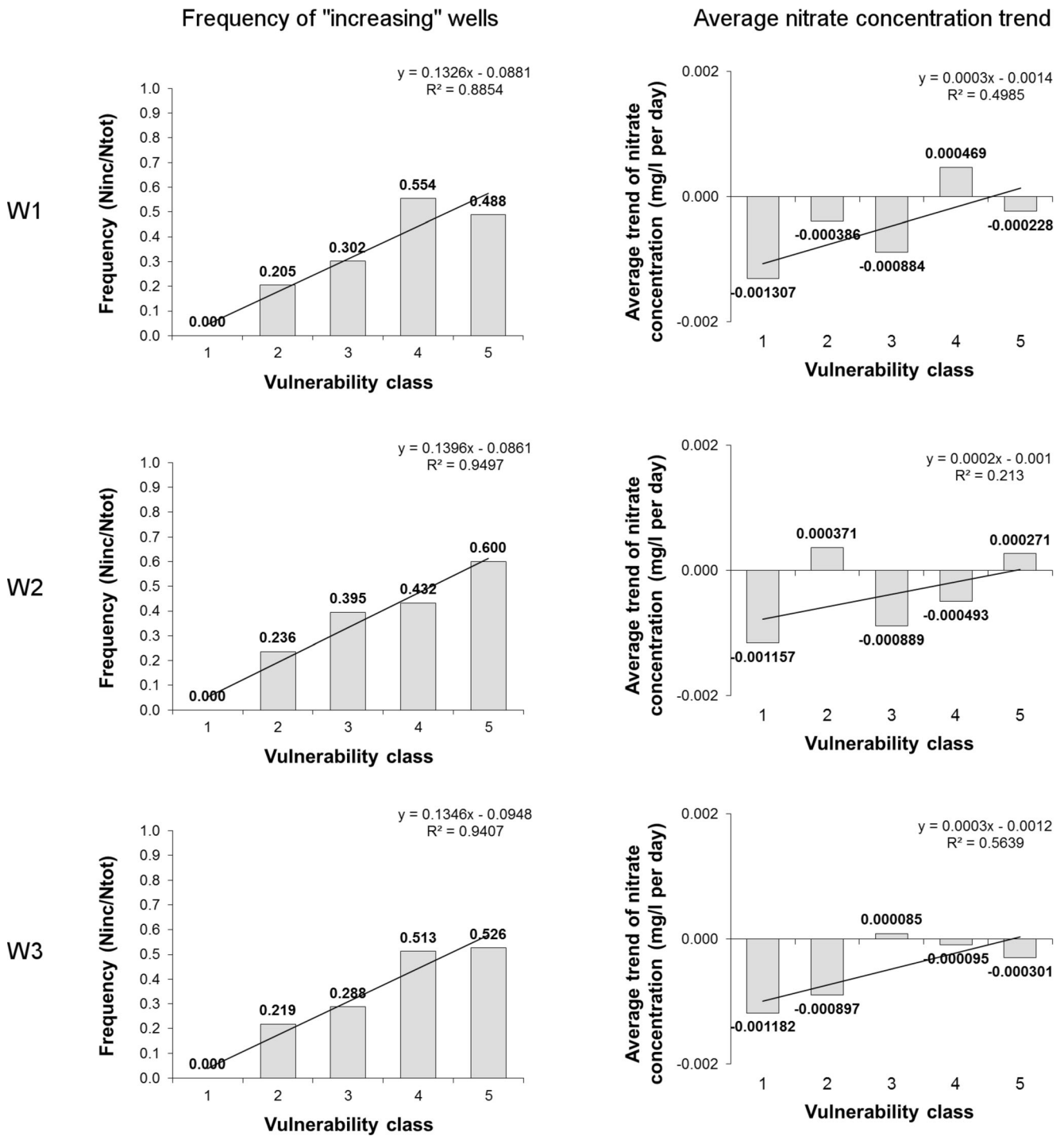


Fig. 10 Histograms of the frequency of the “increasing” wells (*left*) and of the average nitrate concentration trend (*right*) in each vulnerability classes of the maps in Fig. 9. The degree of vulnerability increases from class 1 to class 5

focal application applied to the binary land-use categorization in the DUSAF maps: small changes in urban extent cannot be accurately detected in large urban areas.

Discussion

The direct correlation for all of the three anthropogenic evidential themes means that increasing nitrate

concentration is related to areas of urban development or population increase, in agreement with Stevenazzi et al. (2014). The three urban variables consistently identify that the most important changes are clustered around the biggest cities or in the northern sector where cities and industries in the Lombardy region are mostly located, while the southern sector primarily consists of agricultural fields. There are anomalies in population density changes

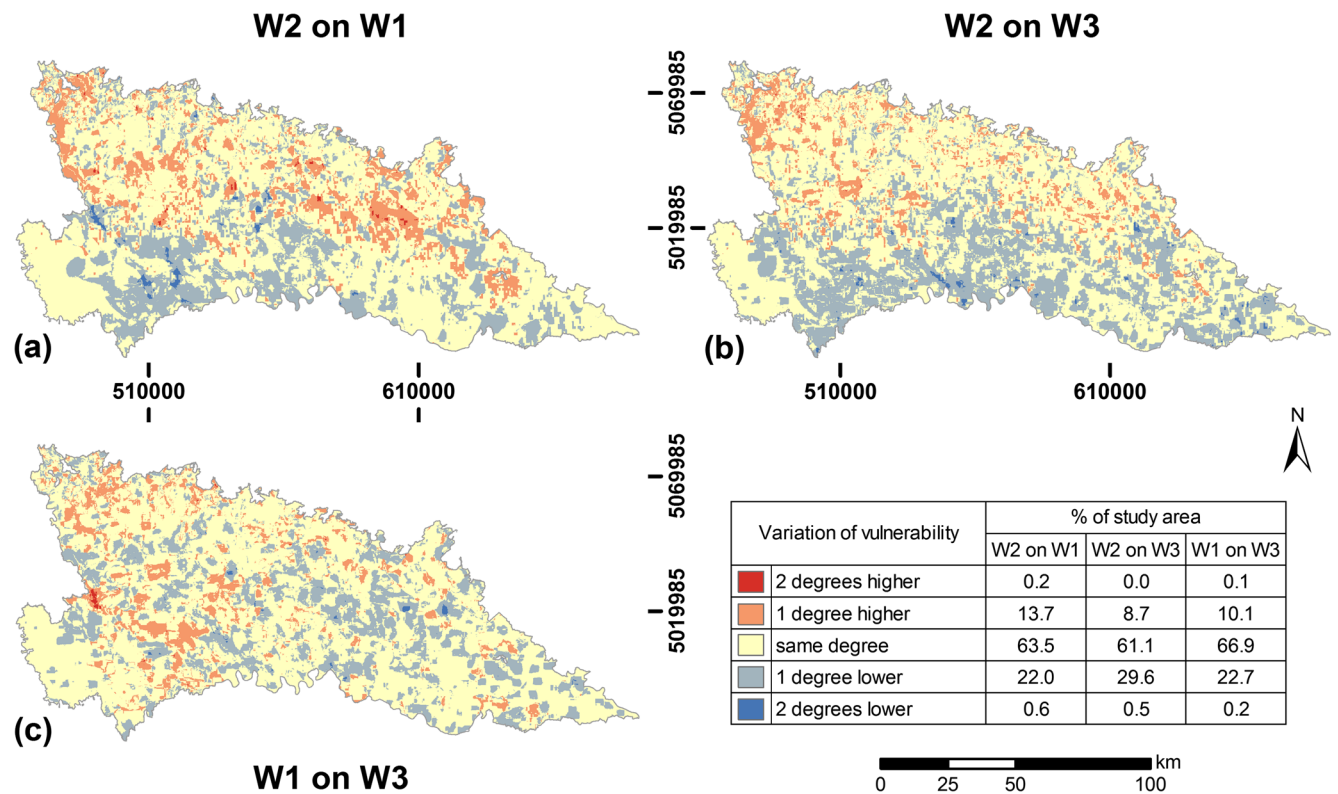


Fig. 11 Variation of vulnerability from map-to-map: **a** map W2 on map W1; **b** map W2 on map W3; **c** map W1 on map W3. The variation is expressed as the agreement in percentage between the vulnerability depicted in the first map with respect to the one depicted in the second map. Coordinates refer to WGS 1984 – UTM Zone 32 N projection

because some sectors in large cities have decreasing trends while small towns show significantly increasing trends. These changes indicate a tendency that people like to move away from over-crowded urban areas and sprawl to more open suburban areas with natural or agricultural surroundings (EEA 2006).

The direct relationship between groundwater depth and increasing concentration trends is consistent with earlier static observations for shallow aquifer in USA (Nolan 2001; Nolan et al. 2002) and in the Province of Milan (Sorichetta et al. 2013). The explanation can be found in bio-geochemical conditions of the vadose zone. In fact, a very shallow water table leads to waterlogged conditions conducive to denitrification processes, in which denitrification rates tend to decrease as water-table depth increases. The result in this study supports this hypothesis and indicates that nitrate concentration changes are related to bio-geochemical activities in the vadose zone.

Groundwater velocity and hydraulic conductivity of the vadose zone are two hydrogeological variables that influence the movements of contaminants from surface to aquifers and within aquifers. The first controls transport and dilution of contaminants within aquifers, and the latter controls the rate at which a contaminant can reach groundwater. In terms of increasing concentration trends in the study area, positive correlations mean that the transport process is generally prevalent over the dilution one, both in groundwater and in the vadose zone. Static analyses (Sorichetta et al. 2013) have found that these

variables have positive correlations with the occurrence of high nitrate concentrations. From this study, increasing concentration trends are shown to relate to increasing groundwater velocity or increasing hydraulic conductivity in the vadose zone. Thus, both static and time-dependent analyses confirm the impacts of these hydrogeological factors on the distribution of contaminants, which are necessary to include in groundwater vulnerability assessment.

Vulnerability maps are calibrated and validated. The similarity in calculated high AUC values for maps W1, W2 and W3 asserts the consistent quality of the maps. Histograms of frequency are excellent for all the maps, with a monotonic increase corresponding to higher vulnerability. Nevertheless, according to the criteria used in evaluating the frequency histograms, map W2 can be considered the one that performs best. In fact, it has the highest regression coefficients and the one with the highest frequency of impacted wells in the highest vulnerability class.

Histograms of average nitrate concentration trends show a general positive trend, although with low values. Maps W1 and W3 have the highest angular and regression coefficients, but only map W2 shows the mean positive value in the higher vulnerability class. No map presents the mean or median value of the whole distribution as average concentration trend in the central vulnerability class.

In summary, QSCAT-DSM can be successfully used as a proxy for nitrate contamination from urban sources and,

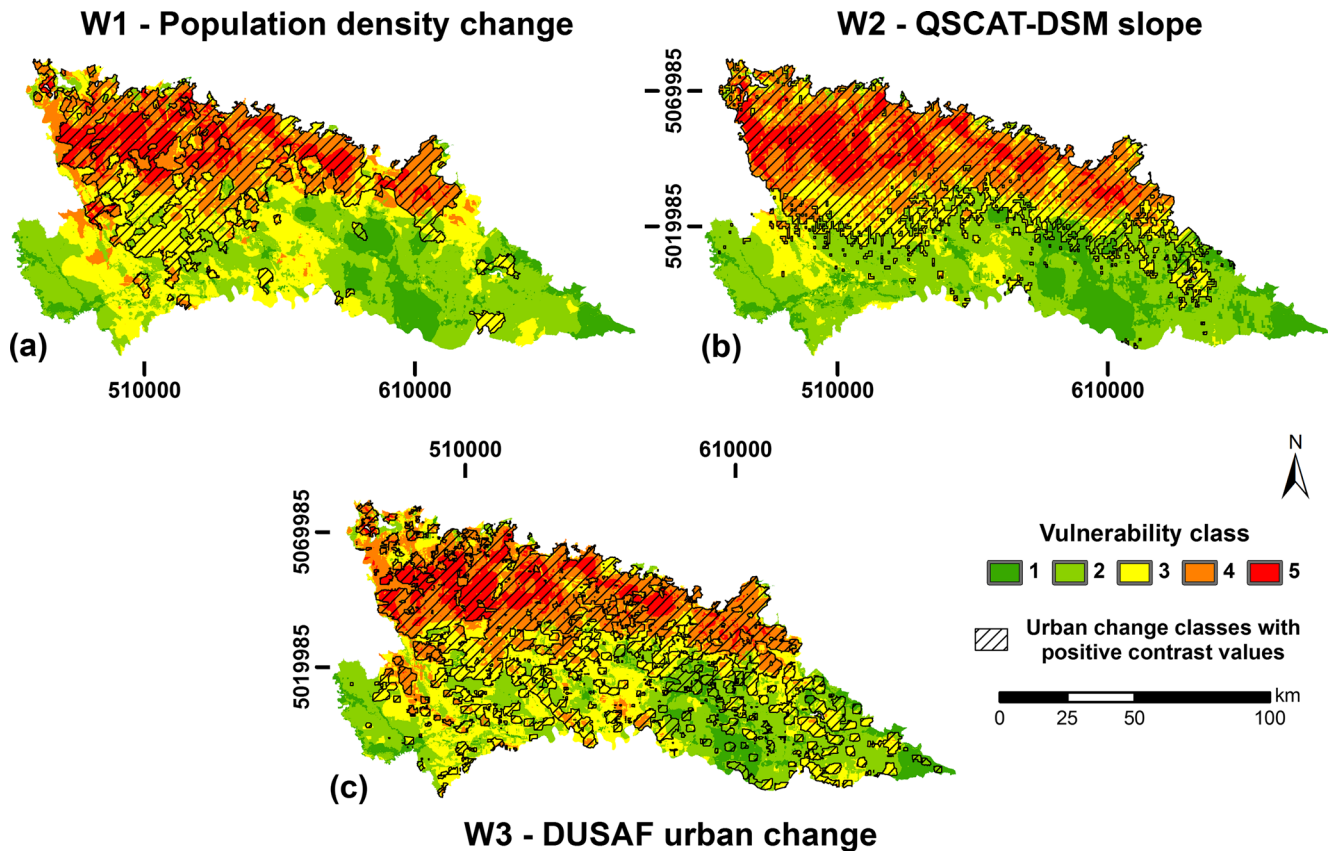


Fig. 12 Vulnerability maps obtained using **a** population density change, **b** QSCAT-DSM slope and **c** DUSAF urban extent change as time-dependent variables, overlain by the corresponding evidential theme classes with positive contrast values. Coordinates refer to WGS 1984 – UTM Zone 32 N projection

among the three obtained vulnerability maps, the map that uses QSCAT-DSM slope to characterize the evolution of urban nitrate sources (map W2) appears to be the best.

Conclusions

Introducing the time variable to monitor trends in groundwater vulnerability assessment is an innovative approach to study the evolution of non-point-source pollution in an area and to forecast future changes.

With the application of a Bayesian spatial statistical approach, it is found that:

- Natural factors, such as groundwater depth, groundwater velocity and hydraulic conductivity of the vadose zone, influence groundwater vulnerability, confirming results from previous studies on nitrate contamination (Nolan 2001; Sorichetta et al. 2013).
- The innovative use of QSCAT-DSM satellite data (Nghiem et al. 2009) in the analysis enables the production of a time-dependent vulnerability map, which is compared with two other vulnerability maps obtained using different time-dependent factors related to urban changes (i.e., population density from census

and changes in land use derived from the DUSAF database).

- All of the time-dependent factors indicate that increasing nitrate concentration occurs in areas related to urban development or population increase.
- The calibration and validation procedures affirm all of the three vulnerability maps have a high reliability, while the one obtained with QSCAT-DSM is the better one.

The latter result is remarkable for those areas where there are insufficient or inaccurate data for population or land use and their changes, and thus satellite observations of urban change become particularly useful. Moreover, QSCAT-DSM data have the advantages of a worldwide coverage, a continuous data collection and an adequate resolution without spatial gaps.

In conclusion, the approach developed in this study for the first time allows the inclusion of the time variable in groundwater vulnerability assessment with the use of innovative remote sensing data to carry out a quantitative statistical analysis of groundwater quality changes.

New approaches to combine groundwater vulnerability maps obtained by explicitly accounting for the time variable with traditional vulnerability maps should be advanced for better intervention strategies and for more

efficient policy measures. Indeed, their combined use would allow one to not only identify already highly contaminated areas where expensive reactive remediation measures need to be implemented, but also to detect areas where pro-active interventions need to be planned. With the method demonstrated in this study, existing and future satellite scatterometer data can be used to make and update maps of groundwater vulnerability as urbanization accelerates across the world.

Acknowledgements The research carried out at the Jet Propulsion Laboratory (JPL), California Institute of Technology, was supported by the National Aeronautics and Space Administration (NASA) Land-Cover and Land-Use Change (LCLUC) Program. We thank Gregory Neumann of JPL for processing satellite QSCAT-DSM data. The research carried out at the Department of Geography and Environment, University of Southampton (UK), was done in the framework of the WorldPop Project (www.worldpop.org.uk) and supported by funding from the Bill & Melinda Gates Foundation (OPP1106427, 1032350).

References

- Al Saud M (2010) Mapping potential areas for groundwater storage in Wadi Aurnah Basin, western Arabian Peninsula, using remote sensing and geographic information system techniques. *Hydrogeol J* 18(6):1481–1495. doi:10.1007/s10040-010-0598-9
- Alberti L, De Amicis M, Masetti M, Sterlacchini S (2001) Bayes' rule and GIS for evaluating sensitivity of groundwater to contamination. In: Proceedings of the International IAMG Conference, Cancun, Mexico, September 2001
- Aller L, Bennet T, Lehr JH, Petty RJ (1987) DRASTIC: a standardised system for evaluating groundwater pollution potential using hydrologic settings. US EPA Report, 600/2-87/035, "Robert S. Kerr" Environmental Research Laboratory, Ada, OK
- Anderson M, Woessner W (1992) Applied groundwater modeling: simulation of flow and advection transport. Academic, San Diego
- Bonham-Carter GF (1994) Geographic information systems for geoscientists: modelling with GIS. Pergamon, New York
- Brunner P, Hendricks Franssen H-J, Kgotlhang L, Bauer-Gottwein P, Kinzelbach W (2007) How can remote sensing contribute in groundwater modeling? *Hydrogeol J* 15(1):5–18. doi:10.1007/s10040-006-0127-z
- Cowan N (2001) The magical number 4 in short-term memory: a reconsideration of mental storage capacity. *Behav Brain Sci* 24:87–185. doi:10.1017/S0140525X01003922
- Doerfliger N, Zwahlen F (1997) EPIK: a new method for outlining of protection areas in karst environment. In: Günay G, Johnson I (ed) Proceedings 5th International symposium and field seminar on karst waters and environmental impacts, Antalya, Turkey. Balkema, Rotterdam, The Netherlands, pp 117–123
- EEA (European Environment Agency) (2006) Urban sprawl in Europe: the ignored challenge (EEA report no. 10/2006). Office for Official Publications of the European Communities, Luxembourg, no. 56, pp 1725–9177
- Eckardt DA, Stackelberg PE (1995) Relation of groundwater quality to land use on Long Island, New York. *Ground Water* 33(6):1019–1033
- ERSAF (Ente Regionale per i Servizi all'Agricoltura e alle Foreste) (2014) DUSAF (Destinazione d'Uso dei Suoli Agricoli e forestali) [Land use database]. <http://www.cartografia.regione.lombardia.it/>. Accessed 30 January 2014
- ESRI (Environmental Systems Research Institute) (2008) ArcGIS Desktop 9.3, Redlands, CA. <http://www.esri.com/software/arcgis/arcgis-for-desktop>. Accessed 14 January 2014
- EuroGeoSurveys (2014) Water Resources. <http://www.eurogeosurveys.org/topics/water-resources>. Accessed 30 July 2014
- European Community (1991) Council Directive 91/676/EEC concerning the protection of waters against pollution caused by nitrates from agricultural sources (Nitrate Directive). *Off J Eur Comm* 375:1–8
- European Community (2006) Directive 2006/118/EC on the protection of groundwater against pollution and deterioration (Groundwater Directive). *Off J Eur Comm* 372:19–31
- Focazio MJ, Reilly TE, Rupert MG, Helsel DR (2002) Assessing ground-water vulnerability to contamination: providing scientifically defensible information for decision makers. US Geol Surv Circ 1224
- Foster SSD (1987) Fundamental concepts in aquifer vulnerability, pollution risk and protection strategy. In: Duijvenbooden W van, Waegeningh HG van (eds) Vulnerability of soil and groundwater to pollutants. NOASR TNO, Delft, The Netherlands, pp 69–86
- Frappart F, Papa F, Güntner A, Werth S, Santos da Silva J, Tomasella J, Seyler F, Prigent C, Rossow WB, Calmant S, Bonnet M-P (2011) Satellite-based estimates of groundwater storage variations in large drainage basins with extensive floodplains. *Remote Sens Environ* 115(6):1588–1594. doi:10.1016/j.rse.2011.02.003
- ISTAT (Istituto di Statistica Applicata al Territorio) (2001) 14° general population and housing census. <http://dawinci.istat.it/>. Accessed 19 March 2013
- ISTAT (Istituto di Statistica Applicata al Territorio) (2011) 15° general population and housing census. <http://www.istat.it/>. Accessed 19 March 2013
- Jasmin I, Mallikarjuna P (2011) Review: Satellite-based remote sensing and geographic information systems and their application in the assessment of groundwater potential, with particular reference to India. *Hydrogeol J* 19(4):729–740. doi:10.1007/s10040-011-0712-7
- Jha MK, Chowdary VM (2007) Challenges of using remote sensing and GIS in developing nations. *Hydrogeol J* 15(1):197–200. doi:10.1007/s10040-006-0117-1
- Jha MK, Chowdary VM, Chowdhury A (2010) Groundwater assessment in Salboni Block, West Bengal (India) using remote sensing, geographical information system and multi-criteria decision analysis techniques. *Hydrogeol J* 18(7):1713–1728. doi:10.1007/s10040-010-0631-z
- Kuroda K, Fukushi T (2008) Groundwater contamination in urban areas. In: Takizawa S (ed) Groundwater management in Asian cities. Springer, Heidelberg, Germany, pp 125–149
- Masetti M, Poli S, Sterlacchini S (2007) The use of the weights-of-evidence modeling technique to estimate the vulnerability of groundwater to nitrate contamination. *Nat Resour Res* 16(2):109–119. doi:10.1007/s11053-007-9045-6
- Masetti M, Poli S, Sterlacchini S, Beretta GP, Facchi A (2008) Spatial and statistical assessment of factors influencing nitrate contamination in groundwater. *J Environ Manage* 86(1):272–281. doi:10.1016/j.jenvman.2006.12.023
- Masetti M, Sterlacchini S, Ballabio C, Sorichetta A, Poli S (2009) Influence of threshold value in the use of statistical methods for groundwater vulnerability assessment. *Sci Total Environ* 407(12):3836–3846. doi:10.1016/j.scitotenv.2009.01.055
- Masetti M, Nghiem SV, Sorichetta A, Stevenazzi S, Bonfanti M, Conforto A, Fabbri P, Filippini M, Gargini A, Hall D, Linard C, Pola M, Richter A, Catani F, Paloscia S, Pampaloni P, Santi E (2014) The Po plain experiment (POPLEX) field campaign: effects of urban sprawl on environmental matrices in northern Italy. *Rend Online Soc Geol It* 31(1):531
- Nghiem SV, Leshkevich GA, Stiles BW (2004) Wind fields over the Great Lakes measured by the SeaWinds scatterometer on the QuikSCAT satellite. *J Great Lakes Res* 30(1):148–165
- Nghiem SV, Balk D, Rodriguez E, Neumann G, Sorichetta A, Small C, Elvidge CD (2009) Observations of urban and suburban environments with global satellite scatterometer data. *ISPRS J Photogramm Remote Sens* 64(4):367–380. doi:10.1016/j.isprsjprs.2009.01.004

- Nghiem SV, Masetti M, Stevenazzi S, Bonfanti M, Conforto A, Filippini M, Fabbri P, Pola M, Sorichetta A, Linard C, Pampaloni P, Palocia S, Santi E, Catini F, Neumann G (2014a) Interdisciplinary study of urbanization and impacts: The POPLEX 2014 Field Campaign, AGU Fall Meeting, San Francisco, December 2014
- Nghiem SV, Sorichetta A, Elvidge CD, Small C, Balk D, Deichmann U, Neumann G (2014b) Remote sensing of urban environments: the Beijing case study. In: Njoku E (ed) *Encyclopedia of remote sensing*, Springer, Heidelberg, Germany, pp 869–878
- Nolan BT (2001) Relating nitrogen sources and aquifer susceptibility to nitrate in shallow ground waters of the United States. *Ground Water* 39(2):290–299
- Nolan BT, Hitt KJ, Ruddy BC (2002) Probability of nitrate contamination of recently recharged groundwaters in the conterminous United States. *Environ Sci Technol* 36(10):2138–2145. doi:10.1021/es0113854
- Raines GL (1999) Evaluation of weights of evidence to predict epithermal-gold deposits in the Great Basin of the Western United States. *Nat Resour Res* 8(4):257–276
- Raines GL, Bonham-Carter GF, Kamp L (2000) Predictive probabilistic modeling using ArcView GIS. *ArcUser* 3(2):45–48
- Regione Lombardia, Eni Divisione Agip (2001) *Geologia degli acquiferi Padani della Regione Lombardia [Geology of the Po Valley aquifers in Lombardy Region]*. S.EL.CA., Florence, Italy
- Sawatzky DL, Raines GL, Bonham-Carter GF, Looney CG (2009) *Spatial Data Modeller (SDM): ArcMAP 9.3 geoprocessing tools for spatial data modelling using weights of evidence, logistic regression, fuzzy logic and neural networks*. <http://arcscripsts.esri.com/details.asp?dbid=15341>. Accessed 14 January 2014
- Sener E, Davraz A (2013) Assessment of groundwater vulnerability based on a modified DRASTIC model, GIS and an analytic hierarchy process (AHP) method: the case of Egirdir Lake basin (Isparta, Turkey). *Hydrogeol J* 21(3):701–714. doi:10.1007/s10040-012-0947-y
- Sorichetta A (2011) *Groundwater vulnerability assessment using statistical methods*. Università degli Studi di Milano, Academic year 2010, 141 pp. <http://hdl.handle.net/2434/152913>. Accessed 17 November 2014
- Sorichetta A, Masetti M, Ballabio C, Sterlacchini S, Beretta GP (2011) Reliability of groundwater vulnerability maps obtained through statistical methods. *J Environ Manage* 92(4):1215–1224. doi:10.1016/j.jenvman.2010.12.009
- Sorichetta A, Ballabio C, Masetti M, Robinson GR Jr, Sterlacchini S (2013) A comparison of data-driven groundwater vulnerability assessment methods. *Ground Water* 51(6):866–879. doi:10.1111/gwat.12012
- Stevenazzi S, Masetti M, Nghiem SV, Sorichetta A (2014) Use of scatterometer data in groundwater vulnerability assessment. *Rend Online Soc Geol It* 30:45–50. doi:10.3301/ROL.2014.10
- Stuart ME, Chilton PJ, Kinniburgh DG, Cooper DM (2007) Screening for long-term trends in groundwater nitrate monitoring data. *Q J Eng Geol Hydrogeol* 40(4):361–376. doi:10.1144/1470-9236/07-040
- Tesoriero A, Voss F (1997) Predicting the probability of elevated nitrate concentrations in the Puget Sound basin: implications for aquifer susceptibility and vulnerability. *Ground Water* 35(6):1029–1039
- Tweed S, Leblanc M, Webb JA, Lubczynski MW (2007) Remote sensing and GIS for mapping groundwater recharge and discharge areas in salinity prone catchments, southeastern Australia. *Hydrogeol J* 15(1):75–96. doi:10.1007/s10040-006-0129-x
- Van Stempvoort D, Evert L, Wassenaar L (1993) Aquifer vulnerability index: a GIS compatible method for groundwater vulnerability mapping. *Water Qual Res J Can* 18:25–37
- Wang H, Guan H, Gutiérrez-Jurado HA, Simmons CT (2014) Examination of water budget using satellite products over Australia. *J Hydrol* 511:546–554. doi:10.1016/j.jhydrol.2014.01.076
- Welch AH, Westjohn DB, Helsel DR, Wanty RB (2000) Arsenic in ground water of the United States: occurrence and geochemistry. *Ground Water* 38(4):589–604
- Werz H, Hötzl H (2007) Groundwater risk intensity mapping in semi-arid regions using optical remote sensing data as an additional tool. *Hydrogeol J* 15(6):1031–1049. doi:10.1007/s10040-007-0202-0
- Worrall F, Besien T (2005) The vulnerability of groundwater to pesticide contamination estimated directly from observations of presence or absence in wells. *J Hydrol* 303:92–107. doi:10.1016/j.jhydrol.2004.08.019